

# Creation of a Dual Chamber Micropump using Rapid Prototyping

Alejandro Acevedo  
California Lutheran University

Rapid Prototyping Center  
Milwaukee School of Engineering  
1025 North Broadway  
Milwaukee, WI 53202-3109. USA

Faculty Advisor: Dr. Larry Fennigkoh

## Abstract

In this paper, we present the realization of a dual layer micropump capable microfluidic systems control. Traditional micropump fabrication techniques require the lamination of etched silicon wafers for the creation of micron size fluid channels. The presented micropump uses the additive manufacturing process of rapid prototyping to eliminate multiple material layers for microchannel formation. The pump consists of two 20 x 50 x 2.7 mm Accura® S110 ultraviolet-photocured layers, four internal diffuser/nozzle elements, two parallel actuation chambers, and an encapsulated rare earth magnet in a silicone membrane for actuation. The driving force is generated by a 4.5Volt 3500 RPM commercially available DC motor with two magnets glued to each side of the shaft. A maximum pumping rate of 2.9mL/min for deionized water was achieved at the input power of 168.5mW.

**Keywords:** Micropump; Nozzle/Diffuser; Rapid Prototyping; Stereolithography; Magnetic Actuation

## 1. Introduction

The emergence of Microelectromechanical systems (MEMS) has enabled a wide range of microfluidic systems control for the delivery of small quantities of fluids. Van Lintel *et al.* [1] presented the first piezoelectric actuated silicon micropump. Since then, the majority of reported silicon based micropumps use piezoelectric actuation, [2], [3]. With the growing importance of genomic, proteonomics, the delivery of medical drugs[3], and emergence of Lab on Chip (LOC) systems, new microfabrication technologies for the realization of diversified actuation methods, and valving principles have been explored. For example, C. Yamahata *et al* [4] used powder blasting microfabrication to create a multiple layer plastic ferrofluidic piston pump actuated by an external rare earth magnet.

Reciprocating micropumps are generally characterized by an actuated membrane, two unidirectional valves, and a single pumping chamber. In diaphragm pumps the actuated membrane causes a periodic change of volume to be converted into a pulsed flow. Pulsed flow is caused by a periodic stop and sudden burst of fluid movement through the outlet valve, supply mode and pump mode, respectively. A variety of actuation mechanisms and valving systems provide the principles for controlled fluid movement. Such actuation mechanisms include piezoelectric [5], electrostatic [6], and electromagnetic [7]. Recent studies of reciprocating micropumps have explored magnets encapsulated in membranes. Actuation is provided by an electromagnetic [4, 7] or an electric motor with embedded magnets on the shaft [8]. Adopted valving systems include passive check valves [7], valveless rectification [8, 9], and ball check valves [8 T pan]. Regardless of actuation mechanism and valving system chosen, pulsating flow is present within reciprocating pump designs. A. Olsson *et al* [10] discussed the parallel arrangement of a double chamber diffuser pump. Such a pump contains two pumping chambers and one actuated membrane. The parallel arrangement of pumping chambers reduces pulsating flow by simultaneously creating a supply mode in one pumping chamber, and a pump mode in the other. Theoretically, the pumping rate of such a pump would be twice that of a pump with a single pumping chamber [10].

There are advantages and disadvantages associated with the many manufacturing techniques used for the creation of micropumps. Refer to [3] for a review of the techniques and characterizations of such micropumps. The technique of Rapid Prototyping (RP) for the creation of microfluidic systems is relatively unknown. One of the few studies of

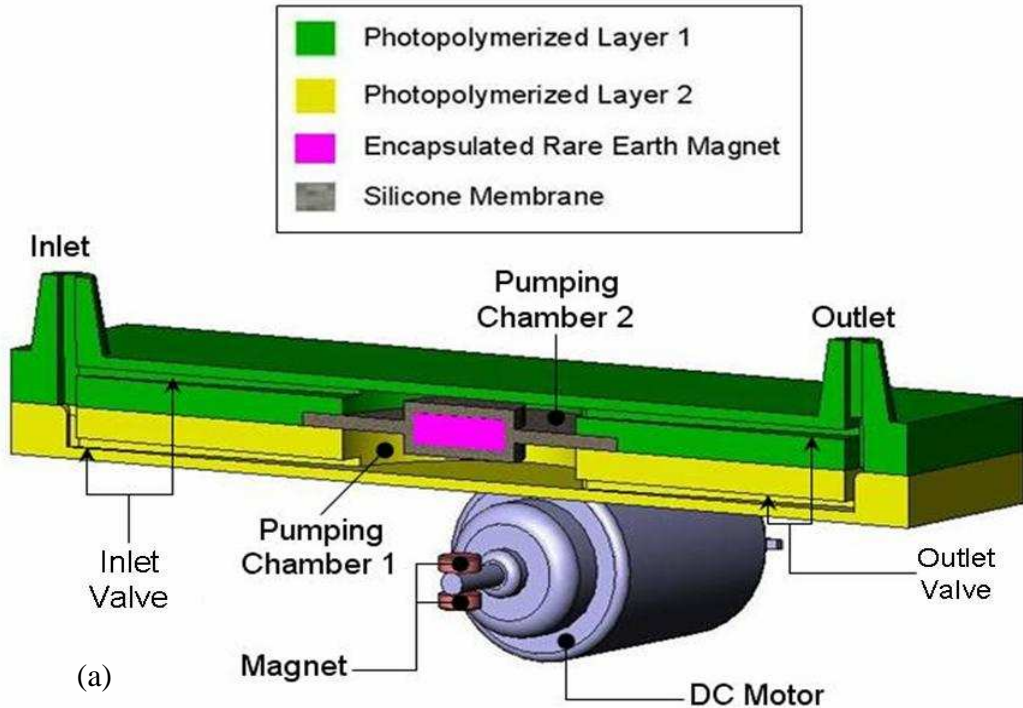
RP used microfluidic control was conducted by M.C. Carrozza *et al* [11] on a piezoelectric micropump fabricated by stereolithography (SLA). RP is an additive manufacturing process allowing the creation of solid objects directly from CAD files. The additive nature of RP allows the fabrication of hidden geometric channels, less restriction of channel curvatures, and the possibility for greater fluid flow control i.e. laminar v.s. turbulent. In addition, RP reduces the layer lamination processes associated with silicon LOC designs.

In this paper we present the realization a three dimensional (3D) microfluidic pump. The pump consists of parallel pumping chambers fabricated on two photopolymerized pump bodies, valveless rectification, and an encapsulated rare earth magnet in a silicone membrane. Actuation of the parallel pumping chambers is provided by a rotating electric motor fitted with bonded magnets on the shaft. Flow rates of 2.9mL/min and backpressures up to 54mm of H<sub>2</sub>O were achieved.

## 2. Working Principle and Design

The micropump is based on the reciprocating motion of a flexible diaphragm to periodically and simultaneously increase and decrease two parallel pumping chamber volumes (Fig 1a). The pump has two parallel pumping chambers actuated by a single silicone membrane with an encapsulated magnet. Fluid displacement is achieved by an electric motor with two  $\varnothing 6.35$  magnets glued on the rotating shaft.

Two diffuser/nozzle elements are located in each micropump layer (Fig 1b). The nozzle/ diffuser element lengths and widths are scaled 5, 4 times larger, respectively, than S.M. Sze *et al* [12] reported for a piezoelectric micropump. The diffuser/nozzle elements are of the flat walled type with length (L) 15mm, depth 0.5mm, inlet width ( $w_1$ ) 0.48mm, outlet width ( $w_2$ ) of 2.56mm, and a nozzle to diffuser angle ( $\theta$ ) of 7.93°. The nozzle/diffuser element contains one rounded corner (curvature  $r=4$ mm) causing the nozzle element to be 1.26mm ( $w_3$ ); all other nozzle/diffuser corners are sharp. Pumping chamber diameter ( $P_d$ ) is 14mm (Fig 1b).



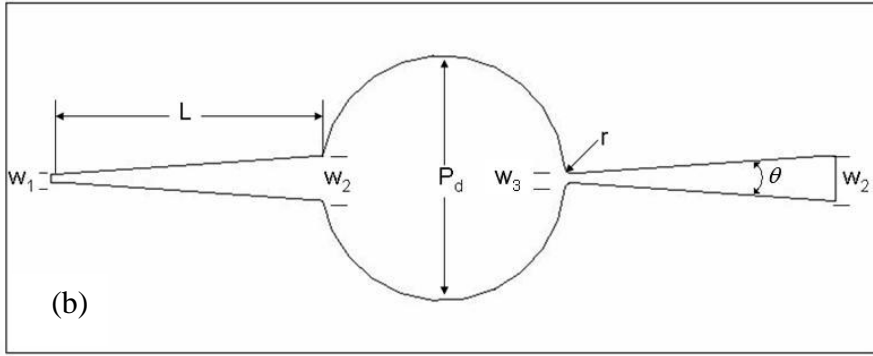


Fig. 1. (a) Schematic diagram of two parallel pumping chambers actuated by external electromagnets. (b) Geometric parameters of the nozzle/diffuser elements; one set per layer.

### 3. Fabrication of the Micropump

#### 3.1. Stereolithography

A 3D Microsystems stereolithography machine, SLA® 5000, fitted with a solid state frequency .01 inch diameter laser fabricated the pump bodies and the microchannels from a CAD file. Accura ® SII0 ultraviolet-photocurable polymer resin was used. The stereolithography process requires supports during normal construction. For the creation of unobstructed microchannels, interior supports were removed during set-up, and the pump was arranged to minimize support interference. To increase the resolution of the fabricated microchannels small feature preserving compensation was chosen. Layer thickness was adjusted to .005 inch layers and the laser scanning speed was program defined.

Once the pump body is fabricated, the parts are placed in an agitating tank filled with Tripropylene Glycol Methyl Ether (TPM) solvent to remove excess resin and weaken exterior support structures. Exterior support structures are then removed, and denatured Alcohol 190 is used to remove resin from the microchannels. Cleaned pieces are then placed in a Post Cure Apparatus (PCA) fitted with a UV light to for 10 minutes.

#### 3.2. Valveless Rectification Formation

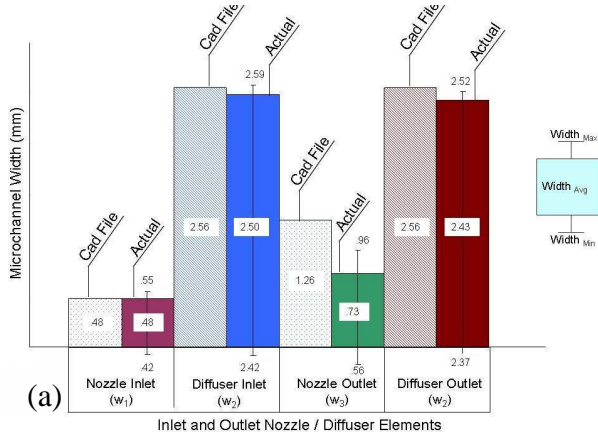
Formation of the defined nozzle/diffuser parameters is important for net fluid movement and pressure buildup. The average, maximum and minimum nozzle/diffuser measurements of five different micropump layers ( $n=10$ ) were used to compare valveless rectification channel formation. Measurements of the fabricated nozzle/diffuser widths ( $w_1, w_2, w_3$ ), length ( $L$ ) and pumping chamber diameter ( $P_d$ ) were conducted on an optical comparator. Gathered measurements were then compared to the dimensions of the computer aided model (CAD) micropump file (Fig. 2.). The collected data indicates the nozzle width of the outlet valve ( $w_3$ ) contains the greatest error. The remaining nozzle/diffuser data indicates a consistent formation of the valveless rectification channels. A greater sample population is needed to confirm the former conclusions.

#### 3.2. Silicone Membrane with Embedded Magnet and actuation mechanism

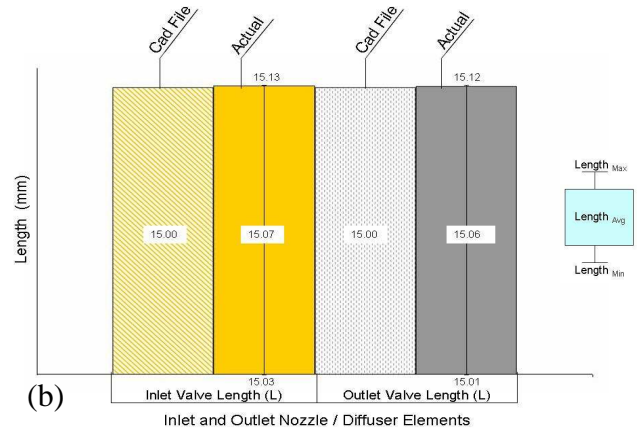
A commercially available  $\varnothing 4.9 \times 1.5$ mm rare earth magnet is encapsulated in a silicone membrane. The membrane negative is created in polycarbonate Lexan® fabricated by normal CNC techniques (Fig. 3a). The molding process relies upon a two step flip over mold. Initially the magnet is placed in the center of the membrane mold, then, degassed Rhodosil® V-340 CA-55 silicone is poured atop the magnet and compressed between two mold halves. After the silicone is cured, one mold half is removed and rotated 180°. To complete the membrane, degassed silicone is poured atop the exposed magnet (Fig. 3b) and compressed between the mold halves. The constructed silicone membrane has an external diameter of 17.53mm (Fig. 3c.).

Two  $\varnothing 6.35 \times 2.54$ mm magnets are glued to the shaft of a commercially available 4.5 Volt 3500 RPM electric motor (Fig. 4.).

### Formation of Valveless Rectification Width



### Formation of Valveless Rectification Length



### Formation of Pumping Chamber Diameter

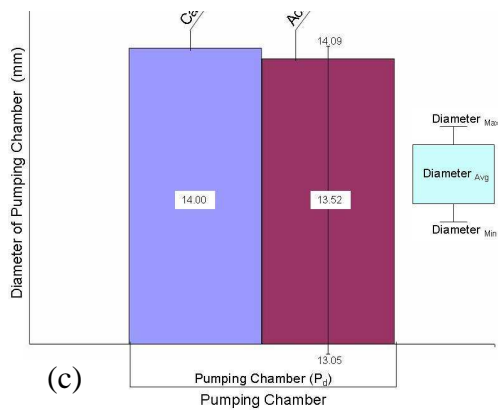


Fig 2. (a) The calculated average, maximum, and minimum width of the inlet and outlet nozzle/diffuser elements ( $w_1, w_2, w_3$ ) plotted against the CAD file width dimensions. (b) The calculated average, maximum, and minimum inlet and outlet nozzle/diffuser length (L) plotted against the CAD file length dimension. (c) The calculated average, maximum, and minimum pumping chamber diameter ( $P_d$ ) plotted against the CAD file pumping chamber diameter dimension.

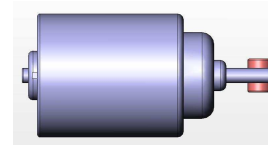


Fig.4. Two rare earth magnets are glued to each side of the motor shaft.

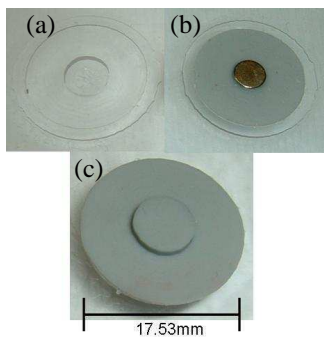


Fig.3. (a) View of the polycarbonate mold. (b) A membrane midway through the fabrication process. (c) A completed membrane with encapsulated magnet.

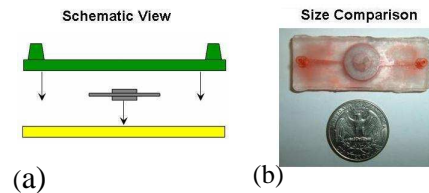


Fig. 5. (a) A burst view of the assembly process. (b) An assembled micropump.

### 3.3. Assembly

Figure 5. depicts the assembly process. The bottom pump body layer contains a one millimeter .4 deep cut extrusion for the silicone membrane to rest upon. The membrane is bonded to the mentioned cut extrusion by Tower Hobbies thick CA glue. To create the closed circuit micropump, glue is applied to the surface of both pump body layers and the outer edges are lined up. Excess glue is minimized to ensure glue does not obstruct the microchannels. Channel interconnectivity between the two layers is checked by passing compressed air through the microfluidic device; however, unobstructed channels are not known until dyed liquid is pumped through the device (Fig. 5b).

### 4. Experimental setup

To standardize the experimental data, the magnets on the motorized shaft were concentrically aligned with the diameter of the encapsulated magnet. Then, the DC motor with bonded magnets on the shaft (actuation device) was glued to an aluminum block, and the micropump was glued to a piece of polycarbonate® Lexan. A distance of 3.83mm was measured between the magnets on the actuation mechanism and the encapsulated magnet in the membrane. At this distance, the encapsulated silicone magnet and glued magnets on the actuation mechanism created a magnetic field of 11.6mT and 72.7mT, respectively. After ensuring the micropump and actuation mechanism were properly secured, rubber hoses with a  $\varnothing$ 2.54mm interior and  $\varnothing$ 3.33mm exterior were connected to the inlet and outlet channels. The free ends of the hoses were placed in DI water.

A 6 volt triple DC power supply provided a variable power source to the DC motor. Different voltage and amperage readings were observed and used to calculate power consumption verses pumping rate and millimeter column heights of water.

### 5. Results

Figure 6. represents the power consumption of the actuation mechanism for a particular pumping rate per minute. The lowest pumping rate reported is 2.5 mL/min at a power consumption of 96.6mW. Lower power wattages were attempted; however, the power was insufficient. The highest pumping rate of 2.9mL/min was achieved at 168.5 mW. Power wattages above 168.9mW were too fast for the magnetic fields to actuate the encapsulated magnet. Consequently, the principles needed for reciprocating micropumps was not met; pumping rate went down and power consumption increased.

Figure 7. represents the power consumption of the actuation mechanism for a particular backpressure. The lowest backpressure is observed at 96.6mW with a 48mm column of H<sub>2</sub>O. The highest pressure observed is at 215.7mW with a 54mm column of H<sub>2</sub>O. Power wattages above 215.7mW were too fast for the magnetic fields to actuate the encapsulated magnet. Consequently, the backpressure reading went down and power consumption increased.

Self priming of the micropump was achieved twice. Countless attempts to repeat self priming were unsuccessful. Additional tests and models are needed to confirm the characterization of the micropump as self priming.

### 6. Conclusion

The results reported provide evidence for the capability of rapid prototyping to produce functional micropumps. Future explorations of the RP manufacturing process could seek to incorporate an encapsulated membrane during the build process. Such endeavors could realize the creation of a micropump in one manufacturing process. Additionally, the successful actuation of the encapsulated magnet adds to the growing research of similar pump designs.

To reach the limits of the dual membrane micropump future research is needed to decrease power consumption, increase pumping rate, and increase backpressure.

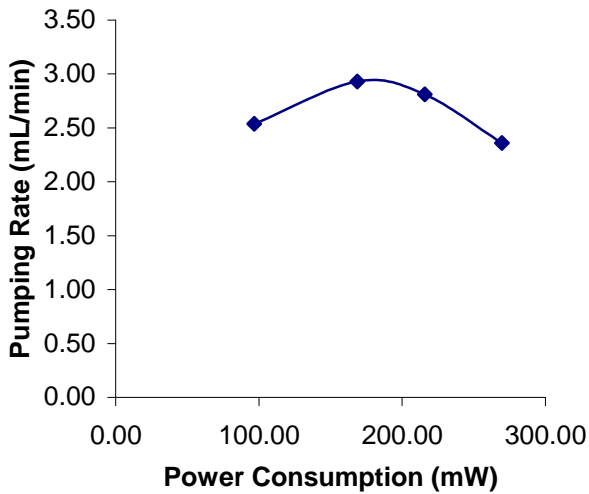


Fig 6. Pumping Rate versus Power Consumption

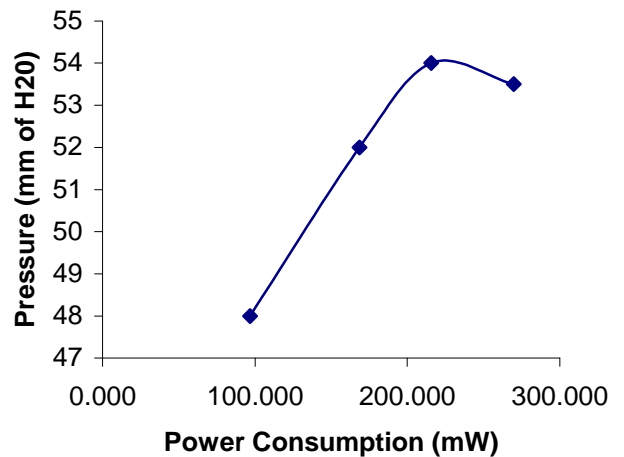


Fig. 7. Backpressure in mm of H<sub>2</sub>O versus Power Consumption

## 5. Acknowledgements

The author wishes to express their appreciation to Larry Fennigkoh for research guidance, Vince Anewenter for his help in constructing the silicone membrane, Elicia Turnbull and Ryan Moore for their stereolithography expertise, and all other workers in the Rapid Prototyping Center. This work is supported by the National Science Foundation, Milwaukee School of Engineering, and the Rapid Prototyping Center.

## 6. References

- [1] H.T.G. van Lintel, F.C.M. van De. Pol, S Bouwstra, Sens. Actuators A 15. (2) (1988) 153-167.
- [2] F.E.H. Tray, W.O. Choong, in F.E.H. Tay (Ed.), Microfluidics and BioMEMS Applications. Boston, MA: Kluwer Academic, 2002, ch1.
- [3] N.T. Nguyen, X. Huang, and T.K. Chuan (2002). "MEMS–Micropumps: A review," *Journal of Fluids Engineering*, 124: 384–392.
- [4] C. Yamahata, M. Chastellain, V.K. Parashar, A. Petri, H. Hofmann, and M.A.M. Gijs., (2005). "Plastic Micropump with Ferrofluidic Actuation," *J. Microelectromechanical Systems*, **14**.
- [5] H.Q. Li, D.C. Roberts, J.L. Steyn, K.T. Turner, J. A. Carretero, O. Yaglioglu, Y.-H. Su, L. Saggere, N.W. Hagood, S.M. Spearing, and M.A. Schmidt, (2000). "A High Frequency High Flow Rate Piezoelectrically Driven MEMS Micropump," *Tech. Dig. Solid-State Sensor and Actuator Workshop*, Hilton Head.
- [6] T. Bourouina, A. Bosseauf and J.P. Grandchamp, (1997). "Design and simulation of an electrostatic micropump for drug-delivery applications," *J. Micromech. Microeng.* **7** 186-188.
- [7] P. Mario, N. Croce, M.C. Carrozza, and G. Varallo, (1996). "A Fluid Handling System for a Chemical Microanalyzer," *J. Micromech. Microeng.*, **6**, 95-98.
- [8] T. Pan, S.J. McDonald, E.M. Kai, Babk Ziaie, (2005). "A magnetically driven PDMS micropump with ball check-valves," *J Micromech. Microeng.* **15** 1021-1026.
- [9] C. Yamahata, F. Lacharme. M.A.M. Gijs., (2005). "Glass Valveless Micropump using electromagnetic actuation." *Microelectronic Eng.* (2005), in print.
- [10] A. Olsson, Ph.D. Thesis: Valve-less Diffuser Micropumps, Royal Institute of Technology, Stockholm, Sweden, 1998
- [11] M.C. Carrozza, N. Croce, B. Magnani, P. Dario, *J. of Micromech. Microeng.* **5** (1995) 177-179.
- [12] S.M. Sze, *VLSI Technology*, 2 ed. New York: McGraw-Hill, 1988.